Supplementary information

Reusing wastewater for agricultural irrigation: a Nexus approach for Sustainable Development in the North Western Sahara Aquifer System

Camilo Ramirez [1], Youssef Almulla [1], and Francesco Fuso-Nerini [1]

[1] KTH Royal Institute of Technology, Stockholm, Sweden

E-mail: camilorg@kth.se

6 July 2020

1. Geographic Information Systems analysis

Geospatial characteristics of the NWSAS were obtained from open sources as described in table 1. All data layers were converted into matching units, re-projected into the Sud Algerie Degree projection (ESRI: 102592)—This projection was selected as it produces

Table 1. Geographic Information System data sources

Layer	Coverage	Format	Resolution	Year	Source
Population	Algeria, Tunisia, Libya	raster (tif)	100 m grid cell	2015	[1]
Depth to groundwater	Africa	txt table	5 km grid cell	2012	[2]
Administrative boundaries	Africa	shapefile	Individual country polygons	2017	[3]
Administrative boundaries	Algeria, Tunisia, Libya	shapefile	Level 1 (provinces) polygons	2015	[4]
Transboundary aquifers borders	Global	shapefile	Individual polygons	2015	[5]
Groundwater quality	NWSAS Basin	data points	206 data points	2016	RA*
Digital Elevation Data*	Africa	raster (tif)	1, 3 and 15 arc second	2014	[6]
Land cover	Africa	raster (tif)	20 m grid cell	2016	[7]
Aquifer boundaries	NWSAS basin	shapefile	Individual polygons	-	RA*
Climate data	Global	raster (tif)	30 arc second, monthly	1970-2000	[8]

* Regional Authorities.

minimal distortions in the analysis area—, re-scaled to the same resolution and, when only individual data points were available, interpolated to extend the data to the entire analysed area (i.e. for the Groundwater quality layer). Furthermore, all layers were merged into a large data frame.

2. Data calibration

The *population* and the *irrigated area* layers were calibrated to match regional statistics. The calibration was performed using the fraction given between the regional statistical data (i.e. total population or total irrigated area), and the sum of all data points of the layer in question. The statistical data was available as per country basis. Thus, the calibration process was performed for the basin areas within each country, using their specific information (see table 2).

Table 2. NWSAS population and irrigated area statistics for year 2015, subdivided per country area inside the basin. Data source: [9]

Parameter	Total	Algeria	Tunisia	Libya
NWSAS Population	6,376,367	4,240,888	617,168	1,518,311
NWSAS Irrigated area (Ha)	469,529	237,485	56,547	175,497

Moreover, to calibrate the irrigated area data, an algorithm was run to ensure that non of the data cells had more than 100% of its area covered by irrigated land.

3. Population and irrigation water withdrawals

The calculation of total water withdrawals $ww_{tot,i}$ was performed according to (1). Population water withdrawals were calculated as the product between the population count in each data cell (Pop_i) and the specific water demand per capita (wpc_i) for the region. Similarly, withdrawals from irrigated agriculture were calculated as the product between the irrigated area inside each data cell ($IrrArea_i$) and the specific water demand per cultivated hectare ($wpha_i$) for the region.

$$ww_{tot,i} = Pop_i \cdot wpc_i + IrrArea_i \cdot wpha_i \tag{1}$$

For the baseline, a level of water withdrawals per capita *wpc* of 55 cubic meters per year was assumed with a population growth of 1% per year [10]. Moreover, all cropland area within the aquifer was considered to be irrigated by groundwater resources and the water requirements per cultivated hectare *wpha* to be 13,520 m^3/Ha for the Algerian part; 13,266 m^3/Ha for Tunisia and 9,134 m^3/Ha for Libya, according to data from [11]. Finally, no growth in irrigated area was considered.

4. Groundwater pumping

The energy needs to pump water from groundwater resources is given by the required lift $(H-h)$, the pressure drop due to fluid friction in the piping, and the pressure losses in valves and fittings. Pressure losses due to friction in the piping were found to be rather small compared to the lift requirements. Therefore, and due to lack of specific data on wells and boreholes in the region, the pressure losses due to friction in the piping and in valves and fittings were disregarded. The energy requirements (in watt-h) can then be estimated as (2) [12]:

$$E = \frac{Q \cdot (\rho \cdot g \cdot (H-h))}{\eta} \tag{2}$$

Where Q stands for the water extractions (m^3), ρ for the water density (kg/m^3), g for the gravitational acceleration (m/s^2), H for the delivered hydraulic head (meters), and h for the head in the well (meters). Moreover, η accounts for the pumping efficiency, which was set as 85% along the entire aquifer.

5. Wastewater Treatment System characteristics

FAO standards for population wastewater pollutant levels and reused water quality for agricultural irrigation [18], were used for the entire NWSAS area. These are shown in table 3.

Table 3. Pollutant levels of wastewater and treated wastewater (mg/l).

Pollutant type	Wastewater	Treated wastewater
Suspended solids (SS)	900	100
Nitrogen (N)	40	10
Phosphorus (P)	20	2
Biochemical Oxygen Demand (BOD_5) (BOD_5)	500	50
Chemical Oxygen Demand (COD)	500	50

Cost functions for different WWTT taken from the work of Molinos-Senante et al. [19], were used to evaluate the competence of selected technologies in the NWSAS. Energy intensity characteristics were added for each technology according to [20, 21]. The characteristics of the different WWTT and their cost and energy functions are presented in table 4.

6. Reverse Osmosis desalination

Reverse Osmosis (RO) desalination is the most popular desalination technology used worldwide. Its energy intensity falls typically in the range of 0.5 to 2.5 kWh per cubic meter of desalinated brackish water [13].

Table 4. Treatment systems analysed. Adapted from [19] unless otherwise stated.

Technology	Contaminants	Costs & Energy	Water
Pond System (PS)	N: 2040 P: 6070 COD: 6096 SS: 5090	CAPEX: $3897.7 \cdot x^{-0.407}$ OPEX: $5.543 \cdot x + 3127.5$ **Energy: $0.19 \cdot V$	Irrigation tailwater
Intermittent Sand Filter (ISF)	N: 6595 P: 7599 COD: 7590 SS: 8595	CAPEX: $2115.5 \cdot x^{-0.399}$ OPEX: $12.026 \cdot x + 3518.9$ **Energy: $0.2 \cdot V$	Population wastewater
Trickling Filter (TF)	N: 3550 P: 3555 COD: 7590 SS: 5090	CAPEX: $12237 \cdot x^{-0.87}$ OPEX: $13.504 \cdot x + 6020$ **Energy: $0.3 \cdot V$	Population wastewater
Moving Bed Biofilm Reactor (MBBR)	N: 1020 P: 3040 COD: 2040 SS: 6080	CAPEX: $1187 \cdot x^{-0.165}$ OPEX: $12.794 \cdot x + 6031$ **Energy: $0.8 \cdot V$	Population wastewater
Rotating Biological Contractors (RBC)	N: 2080 P: 1030 COD: 7093 SS: 7598	CAPEX: $6931.4 \cdot x^{-0.383}$ OPEX: $313.4 \cdot x^{-0.435}$ **Energy: $0.8 \cdot V$	Population wastewater
Membrane Bioreactor (MBR)	N: 5090 P: 2070 COD: 7090 SS: 8599	CAPEX: $5635.3 \cdot x^{-0.352}$ *OPEX: $2.116 \cdot V^{0.713} e^{1.51 \cdot SS + 0.037 \cdot BOD}$ **Energy: $0.8 \cdot V$	Population wastewater
Extended Aeration (EA)	N: 5090 P: 1570 COD: 7090 SS: 8599	CAPEX: $7946 \cdot x^{-0.460}$ *OPEX: $169.48 \cdot V^{0.454} e^{0.61 \cdot SS}$ **Energy: $0.6 \cdot V$	Population wastewater
Sequencing Batch Reactor (SBR)	N: 5590 P: 2570 COD: 7090 SS: 8599	CAPEX: $8258.9 \cdot x^{-0.407}$ OPEX: $309.4 \cdot x^{-0.389}$ **Energy: $1 \cdot V$	Population wastewater

* Taken from [22]

** Based on [23, 21]

x: population equivalent, $x = V \times 1500/(400 \times 365)$, V: wastewater flow (m^3/yr)

To estimate the energy required to desalinate one cubic meter of saline water, often detailed information of the RO system is required. When analysing a broad area using a geospatial approach, such information is not available as the characteristics of the system can change from application to application [15, 16]. Thus, a simplified approach was used to estimate the RO energy requirements. RO is a pressure-driven process that forces water through a membrane which separates dissolved solutes using preferential diffusion. The output water from the membrane (*permeate, p*) is relatively free of solutes, while the remaining water (*concentrate, c*) exits the pressure vessel with

a high concentration of solutes (i.e. high TDS levels). A schematic representation of the process is presented in figure 1 [14].

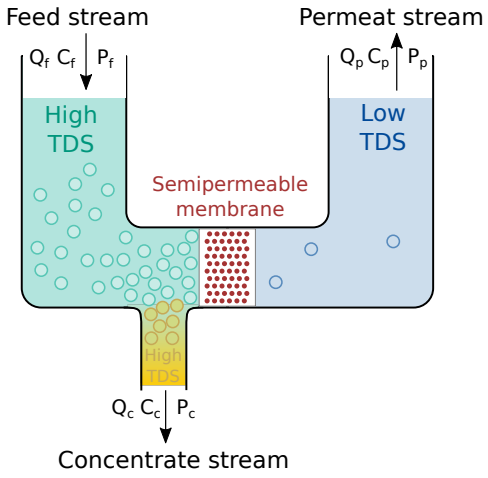

Figure 1. Reverse osmosis schematic separation process. Based on: [14].

The minimum energy required to push the water through the membrane is given by the amount of diluted solutes in the *feed (f)* water. Such minimum energy can be estimated calculating the osmotic pressure of the *feed* water, as described in (3) [14].

$$\pi = \phi \cdot C \cdot R \cdot T \tag{3}$$

Where:

- π: osmotic pressure (bar),
- ϕ: osmotic coefficient, close to 1 (-), assumed a 0.95 [14],
- C: concentration of all solutes (mol/L),
- R: universal gas constant, 0.083145 (L·bar/mol·K),
- T: absolute temperature (K), (273 + °C), assumed at 25 °C for the entire aquifer.

Thus, the minimum energy demand can be estimated multiplying the osmotic pressure of the *feed* water π (in bar) by a conversion factor of 1.0 kWh/m^3 = 36 bar. In reality, the energy demanded is greater due to factors as friction losses, membrane filtration resistance, among others. However, this approach has been used in cases were no specific data of the RO system is available [17].

The water quality layer used, was obtained from 206 measurements provided by National Authorities of the region. Each point specifies the spacial location and groundwater TDS content. Although the data did not covered the entire basin area, due to lack of any other related information it was used to produced a raster layer. An inverse distance weighted interpolation method, having as distance weighting factor an inverse distance to a power of 2 and a global search radius with maximum number of nearest points of 10 was used (see figure 2).

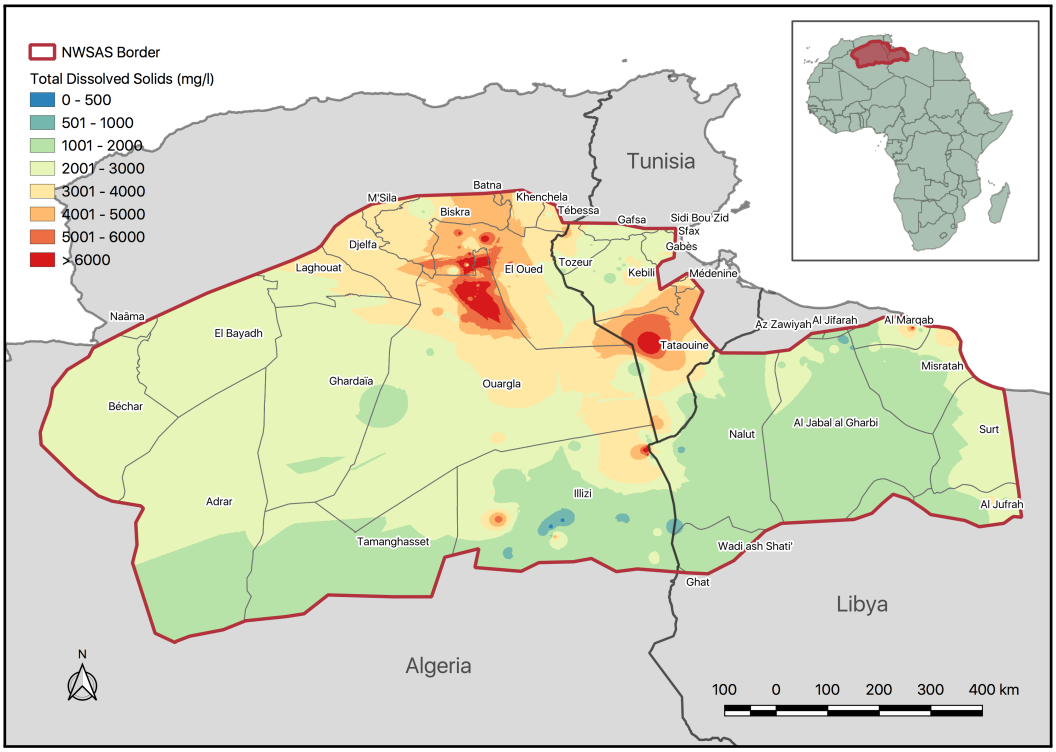

Figure 2. North Western Sahara Aquifer System - Groundwater quality map, Total Dissolved Solids (TDS) at 1×1 km grid cell resolution.

7. Energy-for-wastewater

To calculate the energy-for-wastewater requirements an energy intensity factor was used for each evaluated treatment technology following (4).

$$E_{ww} = Q_{ww,yr} \cdot X_t \tag{4}$$

Where $Q_{ww,yr}$ represents the yearly treated wastewater in m^3/yr, and X_t the average energy demand of the specific WWTT t, to treat one m^3 of wastewater (in kWh/m^3).

References

[1] Catherine Linard, Marius Gilbert, Robert W. Snow, Abdisalan M. Noor, and Andrew J. Tatem. Population Distribution, Settlement Patterns and Accessibility across Africa in 2010. *PLOS ONE*, 7(2):1–8, 2012. doi: 10.1371/journal.pone.0031743.

[2] A M MacDonald, H C Bonsor, B É Ó Dochartaigh, and R G Taylor. Quantitative maps of groundwater resources in Africa. *Environmental Research Letters*, 7(2): 024009, 2012. ISSN 1748-9326. doi: 10.1088/1748-9326/7/2/024009.

[3] Humanitarian Information Unit, United States Government. AfricaAmericas LSIB Polygons Simplified. Technical report, United States Government, 2017.

[4] GADM. Algeria, Tunisia and Libya country boundaries spatial data. `https://gadm.org/index.html`, 2018. Accessed: 2018-08-15.

[5] IGRAC (International Groundwater Resources Assessment Centre). Transboundary Aquifers of the World [map]. Edition 2015. Scale 1 : 50 000 000. `https://gadm.org/index.html`, 2015. Accessed: 2018-08-15.

[6] Jonathan de Ferranti. African Digital Elevation Data. `http://viewfinderpanoramas.org/dem3.html`, 2014. Accessed: 2018-08-15.

[7] ESA Climate Change Initiative - Land Cover project. S2 prototype LC 20m map of Africa 2016. `http://2016africalandcover20m.esrin.esa.int/`, 2017. Accessed: 2018-08-15.

[8] WorldClim - Global Climate Data. http://www.worldclim.org/, 2020.

[9] OSS. *For a Better Valorization of Irrigation Water in the SASS Basin: Diagnosis and Recommendations*. Sahara and Sahel Observatory, 2015. ISBN 978-9973-856-87-6. NWSAS.

[10] Meriem Naimi-Ait-Aoudia and Ewa Berezowska-Azzag. Household water consumption in Algiers facing population growth. Water and Cities, Managing a Vital Relationship. *Proceedings of the 50th ISOCARP Congress, Urban Transformations, Cities and Water*, page 12, 9 2014.

[11] Sahara and Sahel Observatory (OSS). Socio-economic aspects of irrigation in the SASS basin. A better water valorization for sustainable management of the basin. Technical report, Sahara and Sahel Observatory, 2014.

[12] Golam Saleh Ahmed Salem, So Kazama, Shamsuddin Shahid, and Nepal C. Dey. Groundwater-dependent irrigation costs and benefits for adaptation to global change. *Mitigation and Adaptation Strategies for Global Change*, 2017. ISSN 1573-1596. doi: 10.1007/s11027-017-9767-7. External.

[13] James A. Roumasset and Christopher Wada. Energy Costs and the Optimal Use of Groundwater. Allied Social Science Association (ASSA) Annual Meeting, January 3-5, 2014, Philadelphia, PA 161892, Agricultural and Applied Economics Association, 2013.

[14] John C. Crittenden, R. Rhodes Trussell, David W. Hand, Kerry J. Howe, and George Tchobanoglous. *MWH's Water Treatment: Principles and Design*. John Wiley & Sons, Inc., 2012. ISBN 978-1-118-13147-3 978-0-470-40539-0. doi: 10.1002/9781118131473.

[15] Ashlynn S. Stillwell and Michael E. Webber. Predicting the Specific Energy Consumption of Reverse Osmosis Desalination. *Water*, 8(12):601, December 2016. ISSN 2073-4441. doi: 10.3390/w8120601. WOS:000392480200054.

[16] S. Aminfard, F.T. Davidson, and M.E. Webber. Multi-layered spatial methodology for assessing the technical and economic viability of using renewable energy to power brackish groundwater desalination. *Desalination*, 450:12–20, January 2019. ISSN 00119164. doi: 10.1016/j.desal.2018.10.014.

[17] A.J. Karabelas, C.P. Koutsou, M. Kostoglou, and D.C. Sioutopoulos. Analysis of specific energy consumption in reverse osmosis desalination processes. *Desalination*, 431:15 – 21, 2018. ISSN 0011-9164. doi: 10.1016/j.desal.2017.04.006. "Desalination, energy and the environment" in honor of Professor Raphael Semiat.

[18] Robert S Ayers and Dennis W Westcot. *Water quality for agriculture*, volume 29. Food and Agriculture Organization of the United Nations Rome, 1985.

[19] M. Molinos-Senante, M. Garrido-Baserba, R. Reif, F. Hernández-Sancho, and M. Poch. Assessment of wastewater treatment plant design for small communities: Environmental and economic aspects. *Science of The Total Environment*, 427-428: 11–18, 2012. ISSN 00489697. doi: 10.1016/j.scitotenv.2012.04.023.

[20] Pratima Singh, Cynthia Carliell-Marquet, and Arun Kansal. Energy pattern analysis of a wastewater treatment plant. *Applied Water Science*, 2(3):221–226, 2012. ISSN 2190-5495. doi: 10.1007/s13201-012-0040-7.

[21] Renan Barroso Soares. Comparative Analysis of the Energy Consumption of Different Wastewater Treatment Plants. *International Journal of Architecture, Arts and Applications*, 3(6):79, 2017. ISSN 2472-1107. doi: 10.11648/j.ijaaa.20170306.11.

[22] F. Hernández-Sancho, M. Molinos-Senante, and R. Sala-Garrido. Cost modelling for wastewater treatment processes. *Desalination*, 268(1):1–5, 2011. ISSN 0011-9164. doi: 10.1016/j.desal.2010.09.042.

[23] A.K. Plappally and J.H. Lienhard V. Energy requirements for water production, treatment, end use, reclamation, and disposal. *Renewable and Sustainable Energy Reviews*, 16(7):4818–4848, 2012. ISSN 1364-0321. doi: 10.1016/j.rser.2012.05.022.